

Search for giant planets around seven white dwarfs in the Hyades cluster with the Hubble Space Telescope

Wolfgang Brandner,¹★ Hans Zinnecker^{2,3} and Taisiya Kopytova^{4,5,1}

¹Max-Planck-Institut für Astronomie, Königstuhl 17, 69117 Heidelberg, Germany

²Deutsches SOFIA Institut, Universität Stuttgart, Germany

³Universidad Autonoma de Chile, Avda Pedro de Valdivia 425, Santiago de Chile

⁴Division of Medical Image Computing, German Cancer Research Center (DKFZ), 69120 Heidelberg, Germany

⁵Ural Federal University, Yekaterinburg, 620002, Russia

Accepted XXX. Received YYY; in original form ZZZ

ABSTRACT

Only a small number of exoplanets has been identified in stellar cluster environments. We initiated a high angular resolution direct imaging search using the Hubble Space Telescope (HST) and its NICMOS instrument for self-luminous giant planets in orbit around seven white dwarfs in the 625 Myr old nearby (≈ 45 pc) Hyades cluster. The observations were obtained with NIC1 in the F110W and F160W filters, and encompass two HST roll angles to facilitate angular differential imaging. The difference images were searched for companion candidates, and radially averaged contrast curves were computed. Though we achieve the lowest mass detection limits yet for angular separations $\geq 0.5''$, no planetary mass companion to any of the seven white dwarfs, whose initial main sequence masses were $> 2.8 M_{\odot}$, was found. Comparison with evolutionary models yields detection limits of ≈ 5 to 7 Jupiter masses according to one model, and between 9 and $\approx 12 M_{\text{Jup}}$ according to another model, at physical separations corresponding to initial semimajor axis of ≥ 5 to 8 A.U. (i.e., before the mass loss events associated with the red and asymptotic giant branch phase of the host star). The study provides further evidence that initially dense cluster environments, which included O- and B-type stars, might not be highly conducive to the formation of massive circumstellar disks, and their transformation into giant planets (with $m \geq 6 M_{\text{Jupiter}}$ and $a \geq 6$ A.U.). This is in agreement with radial velocity surveys for exoplanets around G- and K-type giants, which did not find any planets around stars more massive than $\approx 3 M_{\odot}$.

Key words: Planets and satellites: gaseous planets – Planets and satellites: formation – Planets and satellites: detection – Planets and satellites: dynamical evolution and stability – white dwarfs – open clusters and associations: individual: Hyades

1 INTRODUCTION

While several 1000 exoplanets and exoplanet candidates have been identified by now (Perryman 2018; Shabram et al. 2020), less than 1% of these reside in stellar clusters (Kovács et al. 2014). Both radial velocity (RV) surveys (e.g., Paulson et al. (2004); Guenther et al. (2005)) and surveys for transiting planets (Gilliland et al. 2000; van Saders & Gaudi 2011; Mann et al. 2016) in populous open and globular cluster confirm the low frequency of close-in planets around cluster members. The RV discovery of a giant exoplanet with $\approx 7.5 M_{\text{Jup}}$ in a ≈ 2 A.U. orbit around the $2.7 M_{\odot}$ K0 giant ϵ Tau, which is a kinematic member of the Hyades open cluster, led to the suggestion that giant planets around intermediate mass stars do exist (Sato et al. 2007).

Direct imaging studies for exoplanets need to overcome both the brightness contrast between a star and its exoplanet, and achieve fine angular resolution in order to separate the exoplanet signal from its host star. Similar to brown dwarfs, planets cool with age and are therefore most easily detectable at young ages while they are still self-luminous in the infrared. Indeed direct imaging searches for

exoplanets have been most successful around young stars (Chauvin et al. 2005; Marois et al. 2008; Lagrange et al. 2009; Macintosh et al. 2015; Chauvin et al. 2017; Keppler et al. 2018).

With the aim to search for giant planets in an open cluster environment, we selected white dwarfs in the Hyades. The Hyades, at an age of 625 ± 50 Myr and at an average distance of 45 pc (e.g., Perryman et al. (1998); Kopytova et al. (2016)), constitute the most nearby open cluster. In addition to 724 stellar systems classified by their proper motion as kinematic member candidates (Röser et al. 2011), seven single white dwarfs (see Table 1) and three white dwarfs, which are companions to stars, have been established as Hyades cluster members (Zuckerman & Becklin 1987; von Hippel 1998). Prior to GAIA DR2 at least six additional white dwarfs were considered likely members of the Hyades cluster (Schilbach & Röser 2012; Tremblay et al. 2012; Zuckerman et al. 2013). Salaris & Bedin (2018) confirm two of these (WD0348+339 and WD0400+148) as high probability members. Born as Herbig Ae stars with initial masses in the range 2.8 to $3.6 M_{\odot}$ (Kalirai et al. 2014), the circumstellar disks of the white dwarf progenitors could have been the birthplaces of giant planets.

White dwarfs offer two advantages for direct imaging surveys for exoplanets (Zinnecker & Friedrich 2001; Burleigh et al. 2002; Gould & Kilic 2008). Firstly, planets on circular or moderately eccentric or-

★ E-mail: brandner@mpia.de

bits with semimajor axis of several A.U. would survive the post-Main Sequence mass loss of the parent star, and would migrate outward adiabatically by a factor equal to the ratio of initial to final stellar mass due to conservation of orbital angular momentum (e.g., [Villaver & Livio \(2009\)](#); [Nordhaus & Spiegel \(2013\)](#)). Secondly, because of their small surface area, white dwarfs are considerably less luminous than their early A- or late B-type main sequence progenitors, thus alleviating the contrast requirements. The reduced contrast requirements facilitated the first direct imaging detection of a brown dwarf as a companion to the white dwarf GD 165 ([Becklin & Zuckerman 1988](#)).

An additional motivation are semianalytic circumstellar disk models by [Kennedy & Kenyon \(2008\)](#), which predict a linear increase in the occurrence rate of giant planets with stellar mass in the range 0.4 to 3 M_{\odot} . Direct imaging detections of giant exoplanets orbiting the mid A-type stars HR 8799 ([Marois et al. 2008, 2010](#)) and β Pic ([Lagrange et al. 2010](#)) might be supportive for these models. With the exception of WD 0806-661 B ([Luhman et al. 2011](#)), direct detection spectroscopic and imaging searches for planetary mass companions to white dwarfs were unsuccessful thus far (e.g. [Chu et al. \(2001\)](#); [Hogan et al. \(2011\)](#); [Xu et al. \(2015\)](#)). Their proximity with distances between 35 and 50 pc ([Bailer-Jones et al. 2018](#)), relatively young age, and main sequence progenitor masses of $\approx 3 M_{\odot}$ make the Hyades cluster white dwarfs promising targets to search for substellar companions at orbital separations of several tens of A.U.

2 OBSERVATIONS AND DATA REDUCTION

The data were obtained with HST/NICMOS (GO 9737, PI H. Zinnecker). Table 1 lists the target sample, basic astrophysical parameters, and the date of the HST observations. The data were obtained with NIC1 in Multiaccum mode (NSAMP=18, STEP32), applying a two point dither pattern with the science targets centered in the top right or bottom right quadrant, respectively, and two telescope roll angles differing by 20 degree. The latter facilitates the application of the angular differential imaging technique for high-contrast subtraction of static PSF structures ([Müller & Weigelt 1987](#); [Lafrenière et al. 2007](#)). Total integration times in F110W and F160W amount to 1280 s and 2560 s, respectively, for each of the white dwarfs.

The raw data were pre-reduced with CALNICA Version 4.4.1. Compared to earlier reductions of this data set ([Zinnecker et al. \(2006\)](#); [Friedrich et al. \(2007\)](#); [Zinnecker & Kitsionas \(2008\)](#)), the re-reduction included a temperature dependent dark correction. This resulted in a better background subtraction, and overall improved contrast ratios in particular at larger angular separations.

The subsequent data reduction steps consisted of

- i pairwise subtraction of dithered positions to remove residual background, and visual inspection for wide companion candidates,
- ii alignment and subtraction of individual 64×64 pixel subfields centered on the white dwarf for two roll angles to facilitate angular differential imaging (removal of static PSF pattern).
- iii Combination and visual inspection of difference frames. Real sources should show up as a positive and negative PSF at the same separation from the white dwarf, and with instrumental position angles differing by 20 degree¹ (see Figure 1).

¹ For WD0421+162 the observations of the 1st HST orbit in F160W are all obtained at the same roll angle. We averaged all observations from this and the 2nd orbit with the same roll angle, and subtracted the one dithered data set obtained in the 2nd HST orbit at the 20 degree offset roll angle.

iv Computation of the residual noise pattern in annuli centred on the white dwarf. The radial 3σ brightest pixel detection limits for each white dwarf are shown in Figure 2.

The contrast curves asymptotically approach the background limit for separations $\geq 0.6''$. At a separation of $0.5''$ the achievable contrast is still subject to PSF residuals. With the exception of WD0406+169, longer exposure times would not have significantly improved the contrast. At angular distances $\geq 0.5''$ from the white dwarf, the detection limit for the full sample is in the range $m_{F110W} = 22.9$ to 23.5 mag and $m_{F160W} = 22.2$ to 22.9 mag. The actual brightness differences (3σ detection limits) at $0.5''$ are $\Delta m_{F110W} = 7.8$ to 8.6 mag, and $\Delta m_{F160W} = 6.7$ to 7.8 mag (see Table 2).

Orbits of confirmed exoplanets with semi-major axis between 4 and 20 A.U. have a mean eccentricity of ≈ 0.35 .² Assuming similar orbital parameters for our sample, we applied a correction factor of 1/0.83 for the conversion from projected separations to semimajor axis (see, e.g., [Leinert et al. \(1993\)](#) for a derivation).

3 FLUX AND MASS DETECTION LIMITS ON EXOPLANETS

Starting from the 3σ Δm_{F110W} and Δm_{F160W} contrast detection limits and the apparent 2MASS J and H magnitudes of the white dwarfs, we calculated the detection limits for companions in terms of apparent magnitudes. The apparent magnitudes were converted to absolute magnitudes using GAIA DR2 parallax measurements for comparison with theoretical evolutionary models for substellar objects.

We selected evolutionary models for substellar objects with solar metallicity by [Baraffe et al. \(2003\)](#) and [Spiegel & Burrows \(2012\)](#). In the latter case, we consider “hybrid” (i.e. a linear combination of cloud and cloud-free) atmospheric models with either high-entropy (hothycl) or low-entropy (coldhycl) initial conditions. For the transformation of brightness limits into mass limits the canonical age of the Hyades of 625 Myr was assumed. It is noted that according to the models even at this relatively advanced age, the most massive exoplanets still retain a “memory” of the starting conditions, i.e. the derived mass estimates assuming a cold start are typically 2 M_{Jup} higher than for a hot start. The presence or absence of atmospheric condensation layers (“DUSTY” or “COND” following the notation by [Allard et al. \(2001\)](#)), and variations of the metallicity result in uncertainties of the same order. As the models by [Spiegel & Burrows \(2012\)](#) are limited to masses $\leq 10 M_{Jup}$, in some cases we used an extrapolation to estimate mass limits.

Also shown in Table 2 are the mass limits derived from SPITZER IRAC observations in the $4.5 \mu m$ band according to [Farihi et al. \(2008\)](#), which are based on the models by [Baraffe et al. \(2003\)](#), and assuming a uniform distance of 46 pc towards all of the white dwarfs.

In all cases, observations in F110W provided lower mass limits, and thus tighter constraints than the observations in F160W. Overall mass limits are in the range of 4.6 to 6.7 M_{Jup} assuming the models by [Baraffe et al. \(2003\)](#). Hybrid clouds and hot start models ([Spiegel & Burrows 2012](#)) place detection limits in the range 8 to 10 M_{Jup} . Thus irrespective of the model set we choose, we should be able to detect brown dwarf companions with masses $\geq 12 M_{Jup}$ at current angular separations $\geq 0.5''$ to any of the seven white dwarfs in the sample. In case the models by [Baraffe et al. \(2003\)](#) are applicable, the average detection limit corresponds to exoplanets with masses in

² <http://exoplanet.eu>

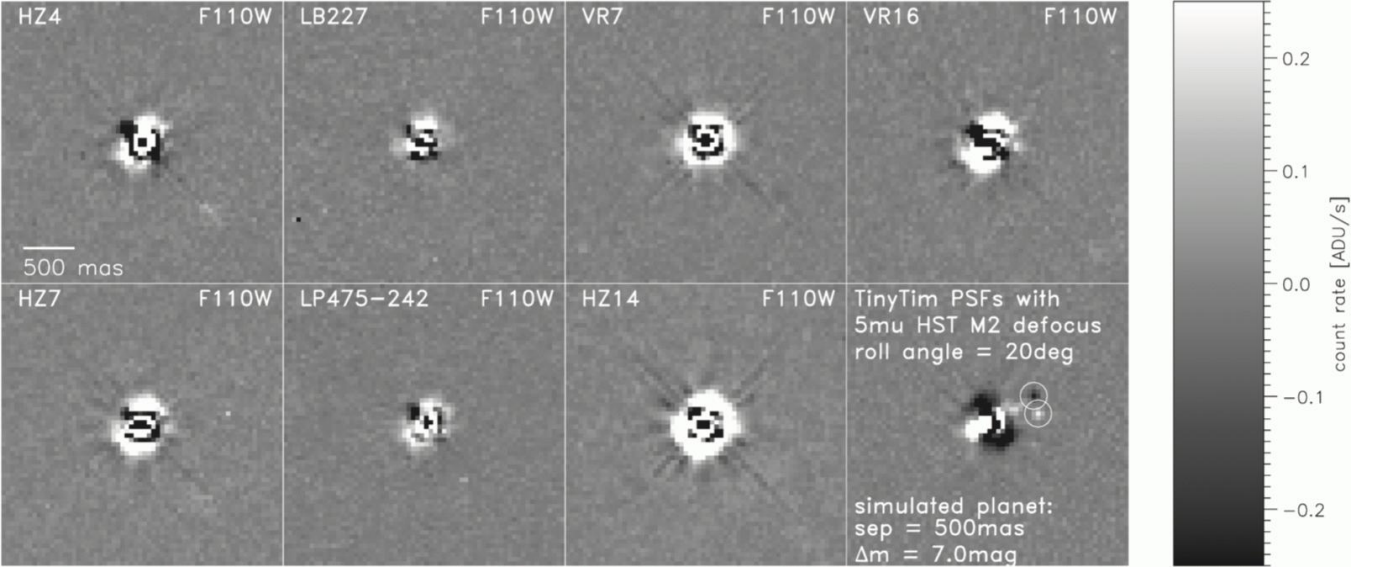


Figure 1. Roll subtracted images of the HST NIC1 observations in F110W of the seven white dwarfs (left to right, top to bottom) and simulated observations based on Tiny Tim PSF simulations (Krist et al. 2011) with an exoplanet at a separation of 500 mas, and 7.0 mag fainter than the white dwarf (lower right).

Table 1. Basic astrophysical parameters of the Hyades single white dwarfs and date of HST/NICMOS observations

name	alt. name	J [mag]	H [mag]	distance [pc]	M_{init} [M_{\odot}]	M_{final} [M_{\odot}]	obs. date
WD0352+096	HZ 4	14.83±0.04	14.87±0.06	35.0	3.59	0.80	2003-11-04
WD0406+169	LB 227	15.70±0.07	15.47±0.12	50.2	3.49	0.85	2004-02-07
WD0421+162	VR 7, LP 415-46	14.75±0.04	14.82±0.06	45.0	2.90	0.70	2004-02-15
WD0425+168	VR 16, LP 415-415	14.63±0.03	14.65±0.05	47.9	2.79	0.71	2003-11-05
WD0431+126	HZ 7	14.77±0.03	14.80±0.06	47.3	2.84	0.69	2003-11-06
WD0437+138	LP 475-242	15.32±0.05	15.51±0.12	46.0	3.41	0.74	2003-11-07
WD0438+108	HZ 14	14.50±0.04	14.62±0.05	49.4	2.78	0.73	2003-11-09

Notes: apparent magnitudes are from 2MASS; distances are based on GAIA DR2 parallaxes (Gaia Collaboration et al. (2016, 2018); Bailer-Jones et al. (2018)), which within the uncertainties are in very good agreement with the distances previously reported by Schilbach & Röser (2012); initial and final mass estimates are from Kalirai et al. (2014)

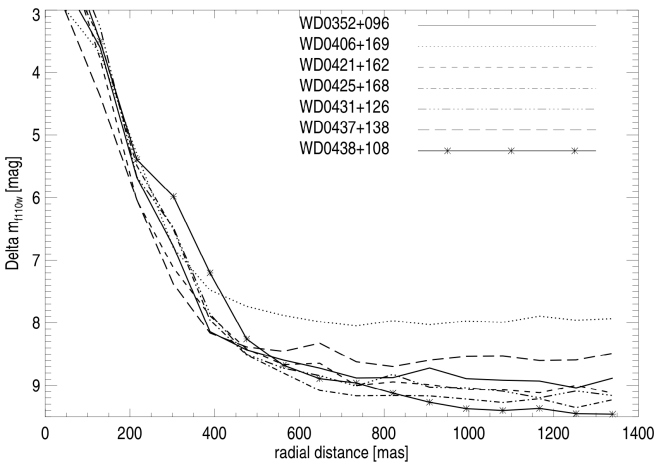


Figure 2. Brightness contrast (3σ) in F110W vs. angular separation for the seven white dwarfs, reaching $\Delta m_{\text{F110W}} > 8$ mag beyond 500 mas).

excess of $\approx 5.6 M_{\text{Jup}}$, which represents an improved detection limit

for resolved exoplanet companions compared to the (indirect) average limit of $\approx 9.4 M_{\text{Jup}}$ from SPITZER/IRAC (Farihi et al. 2008).

4 DISCUSSION

Present-day mass estimates for Hyades white dwarfs have been derived from analysis of spectroscopic data using atmospheric models (Bergeron et al. 2011; Gianninas et al. 2011). We note that gravitational redshift measurements for a subset of the Hyades white dwarfs yield 5% to 10% lower masses estimates (Pasquini et al. 2019). For the following discussion, we consider this small systematic discrepancy in mass estimates of minor importance.

The Hyades white dwarf progenitors lost about 75 % of their initial mass (Kalirai et al. 2014). Due to conservation of orbital angular momentum during the RG/AGB phase any surviving stellar or substellar companion must have migrated outward adiabatically, enlarging the semi-major axis of its orbit by a factor of 3.8 to 4.6 (ratio of initial stellar to final white dwarf mass, see Table 1). Giant planets with initial semi-major axis of their orbits $\gtrsim 5$ A.U. would have survived the post-main sequence mass loss of the parent star (e.g., Villaver & Livio (2009); Nordhaus & Spiegel (2013)), and could now be found in orbits with semimajor axis $\gtrsim 20$ to 30 A.U. The latter corresponds

Table 2. Detection limits at angular separation $\geq 0.5''$ in F110W and F160W: brightness difference, 3σ apparent and absolute magnitude limit, corresponding upper mass limit for substellar companions according to evolutionary and atmospheric models, and current and initial projected physical separation corresponding to $0.5''$ based on mass-loss estimates for the white dwarf progenitors and assuming a typical orbital eccentricity of 0.35. Mass limits at $4.5\ \mu\text{m}$ are from [Farihi et al. \(2008\)](#) and are based on Baraffe models.

name: WD...	0352+096	0406+169	0421+162	0425+168	0431+126	0437+138	0438+108
Δm_{F110W} [mag]	8.48	7.79	8.60	8.59	8.62	8.35	8.39
$m_{\text{lim}F110W}$ [mag]	23.31	23.49	23.35	23.22	23.39	23.67	22.89
$M_{\text{lim}F110W}$ [mag]	20.6	20.0	20.1	19.8	20.0	20.4	19.4
$\text{mass}_{\text{Baraffe}} [M_{\text{Jupiter}}]$	4.6	5.7	5.5	6.2	5.7	4.9	6.7
$\text{mass}_{\text{hothycl}} [M_{\text{Jupiter}}]$	7.7	8.6	8.5	9.0	8.6	8.0	9.6
$\text{mass}_{\text{coldhycl}} [M_{\text{Jupiter}}]$	9.1	10.3:	10.1:	10.8:	10.3:	9.5	11.7:
Δm_{F160W} [mag]	7.74	6.70	7.50	7.80	7.65	7.35	7.63
$m_{\text{lim}F160W}$ [mag]	22.61	22.18	22.31	22.45	22.46	22.86	22.26
$M_{\text{lim}F160W}$ [mag]	19.9	18.7	19.0	19.0	19.1	19.5	18.8
$\text{mass}_{\text{Baraffe}} [M_{\text{Jupiter}}]$	5.9	8.2	7.2	7.2	7.0	6.5	7.8
$\text{mass}_{\text{hothycl}} [M_{\text{Jupiter}}]$	8.3	10.0	9.5	9.5	9.4	8.8	9.8
$\text{mass}_{\text{coldhycl}} [M_{\text{Jupiter}}]$	9.8	12.1:	11.5:	11.5:	11.3:	10.5:	11.9:
$\text{mass}_{4.5\mu\text{m}} [M_{\text{Jupiter}}]$	10	7	10	10	10	8	11
a_{curr} [A.U.]	21	30	27	29	28	28	30
a_{init} [A.U.]	4.7	7.4	6.5	7.3	6.9	6.0	7.8

Notes: we selected models for solar metallicity by [Baraffe et al. \(2003\)](#) and [Spiegel & Burrows \(2012\)](#). In the latter case, the mass estimates are based on models assuming hybrid clouds and either a hot (hothycl) or a cold (coldhycl) start.

":" indicates that the mass limits are based on extrapolation beyond the mass range covered by the models.

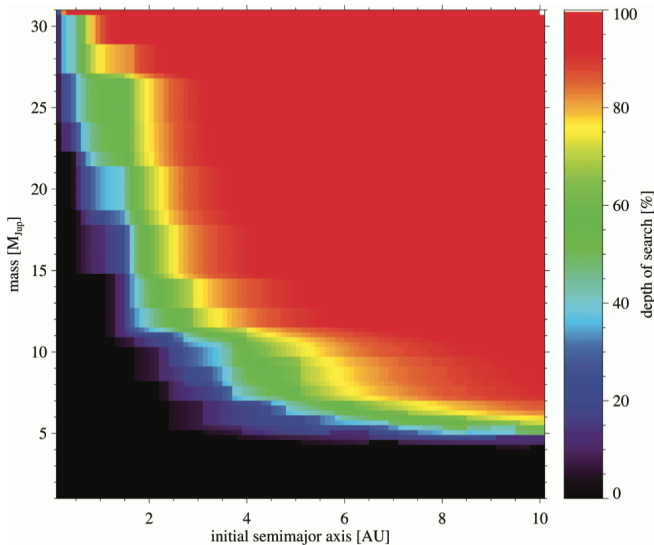


Figure 3. Depth of search, indicating the completeness of the survey of the seven white dwarfs with respect to companion mass and semimajor axis for an assumed typical orbital eccentricity of 0.35. The green colour marks a detection probability of $\approx 50\%$, while the red colour corresponds to $\gtrsim 90\%$.

to angular separations $\geq 0.5''$, which we probe in our HST/NICMOS survey. The present survey does not probe for planets initially in closer orbits (< 2 to 3 A.U.), which during the RG/AGB phase might have merged with the star due to dynamical friction and tidal interactions ([Mustill et al. 2013](#); [Veras et al. 2014](#)).

The NICMOS observations confirm that all seven white dwarfs are single objects. Based on the detection limits and irrespective of evolutionary model we choose, we can rule out brown dwarf companions with masses $\geq 12 M_{\text{Jup}}$ to any of the white dwarfs at current projected separations ≥ 18 to 25 A.U.

Figure 3 visualizes the depth of search of our survey based on the models by [Baraffe et al. \(2003\)](#). We convert radial distances from the contrast curves (Figure 2) into present day physical separations, and initial semimajor axis during the main-sequence phase of the host stars based on the white dwarf mass loss estimates. The detection probabilities were calculated assuming planetary orbits with an eccentricity of 0.35 seen from 8000 uniformly distributed viewing angles and at 126 orbital phases distributed uniformly in time. Compared to a search with SPITZER/IRAC using infrared excess of the white dwarfs as an indicator for unresolved very low-mass companions ([Farihi et al. 2008](#)), our mass limits for resolved giant planets at angular separations ≥ 500 mas are on average $\approx 4 M_{\text{Jup}}$ lower. Our survey reaches a 50% depth of search at $\approx 6 M_{\text{Jup}}$ and for an initial semimajor axis of 6 AU. Ground-based adaptive optics assisted direct imaging surveys for giant exoplanets, which focus on young stars in the solar neighbourhood, in general probe an overlapping part of the parameter space. For stars more massive than $1.5 M_{\odot}$, the GPIES survey at Gemini South ([Nielsen et al. 2019](#)) reaches a 50% depth of search at $\approx 6 M_{\text{Jup}}$ for semimajor axis ≥ 50 AU. The SHINE survey at the VLT ([Vigan et al. 2020](#)) reports for spectral types M to B a 50% depth of survey at $6 M_{\text{Jup}}$ for semimajor axis ≥ 15 to 20 AU.

While our sample of seven single white dwarfs is small, it provides further evidence that initially dense cluster environments, which included O and early B stars, might not be highly conducive for the formation and transformation of massive circumstellar disks around stars with masses $\geq 2.8 M_{\odot}$ into giant planets with semimajor axes ≥ 6 A.U. and with ≥ 6 Jupiter masses. This is in agreement with the radial velocity survey for exoplanets around 373 G- and K-type giants by [Reffert et al. \(2015\)](#), which did not find any planets around giants with initial main sequence masses higher than $2.7 M_{\odot}$. Other high contrast direct imaging searches for planetary mass companions to nearby white dwarfs also did not yield any direct detections ([Debes et al. 2005](#); [Farihi et al. 2005](#); [Debes et al. 2006](#); [Xu et al. 2015](#)) apart from GD165AB.

Indirect evidence for the presence of planets has been derived

from abundance anomalies in white dwarf atmospheres and in their accretion disks as well as from the longevity of debris disks (e.g. Zuckerman et al. (2010, 2013); Farihi et al. (2013); Bergfors et al. (2014); Xu et al. (2019)). Using optical spectroscopy, Gänsicke et al. (2019) reported strong evidence for a photoevaporating giant planet in close ($15 R_{\odot}$) orbit around a hot white dwarf (WD 1145+017); see also an earlier case suggested by Chu et al. (2001). Recently Vanderburg et al. (2020) announced the detection of a transiting giant planet in a 1.4 day orbit around the relatively old WD 1856+534.

In the Hyades, several Earth- to Neptune sized exoplanets and exoplanet candidates transiting K- and M-dwarfs were identified with K2 (Mann et al. 2016; Ciardi et al. 2018; Livingston et al. 2018; Vanderburg et al. 2018). The $2.7 M_{\odot}$ K-giant ϵ Tau still remains the most massive Hyades member known to host a (giant) exoplanet (Sato et al. 2007).

The divergence of mass estimates between the different evolutionary models and the underlying uncertainty about the starting conditions in the formation of substellar objects highlights the importance of testing and calibrating evolutionary models. This requires both independent mass estimates via astrometric or radial velocity reflex motion of the host star, and studies of the early formation phases of exoplanets. ELTs equipped with laser guide star adaptive optics systems could probe the Hyades white dwarfs for giant planets at closer projected separations, and lower mass limits. ELT/MICADO is expected to achieve a contrast of $\Delta H \approx 14.8$ mag at an angular separation of 500 mas (Perrot et al. 2018), and thus (according to the model by Baraffe et al. (2003)) could detect planets with 1 to $2 M_{\text{Jup}}$ orbiting a white dwarf in the Hyades cluster. In the K-band JWST/NIRCam is predicted to achieve a contrast of $\Delta m_{F210M} \approx 11.5$ mag at 500 mas (Beichman et al. 2010), which yields mass detection limits of the same order as the present HST/NICMOS study in F110W (giant planets in the mass and age range under consideration are considerably fainter in the K-band than in the J- and H-bands due to molecular opacities in their atmospheres). The larger collecting area, and improved detector technology of JWST/MIRI relative to SPITZER/IRAC will provide a considerably improved sensitivity for detecting infrared excess from unresolved companions, and might also reach detection limits of 1 to $2 M_{\text{Jup}}$ for the Hyades white dwarfs.

ACKNOWLEDGEMENTS

We thank S. Reffert, S. Röser, J. van Cleve, and S. Xu for helpful comments on a draft of the paper.

Based on observations made with the NASA/ESA Hubble Space Telescope (GO 9737), obtained from the data archive at the Space Telescope Science Institute. STScI is operated by the Association of Universities for Research in Astronomy, Inc. under NASA contract NAS 5-26555.

This publication makes use of data products from the Two Micron All Sky Survey, which is a joint project of the University of Massachusetts and the Infrared Processing and Analysis Center/California Institute of Technology, funded by the National Aeronautics and Space Administration and the National Science Foundation.

This work has made use of data from the European Space Agency (ESA) mission *Gaia* (<https://www.cosmos.esa.int/gaia>), processed by the *Gaia* Data Processing and Analysis Consortium (DPAC, <https://www.cosmos.esa.int/web/gaia/dpac/consortium>). Funding for the DPAC has been provided by national institutions, in particular the institutions participating in the *Gaia* Multilateral Agreement.

DATA AVAILABILITY

The data underlying this article is available online from the Barbara A. Mikulski Archive for Space Telescopes. The final data products will be shared by the corresponding author on request.

REFERENCES

- Allard F., Hauschildt P. H., Alexander D. R., Tamanai A., Schweitzer A., 2001, *ApJ*, **556**, 357
- Bailer-Jones C. A. L., Rybizki J., Foesneau M., Mantelet G., Andrae R., 2018, *AJ*, **156**, 58
- Baraffe I., Chabrier G., Barman T. S., Allard F., Hauschildt P. H., 2003, *A&A*, **402**, 701
- Becklin E. E., Zuckerman B., 1988, *Nature*, **336**, 656
- Beichman C. A., et al., 2010, *PASP*, **122**, 162
- Bergeron P., et al., 2011, *ApJ*, **737**, 28
- Bergfors C., Farihi J., Dufour P., Rocchetto M., 2014, *MNRAS*, **444**, 2147
- Burleigh M. R., Clarke F. J., Hodgkin S. T., 2002, *MNRAS*, **331**, L41
- Chauvin G., et al., 2005, *A&A*, **438**, L29
- Chauvin G., et al., 2017, *A&A*, **605**, L9
- Chu Y.-H., Dunne B. C., Gruendl R. A., Brandner W., 2001, *ApJ*, **546**, L61
- Ciardi D. R., et al., 2018, *AJ*, **155**, 10
- Debes J. H., Sigurdsson S., Woodgate B. E., 2005, *AJ*, **130**, 1221
- Debes J. H., Ge J., Ftaclas C., 2006, *AJ*, **131**, 640
- Farihi J., Zuckerman B., Becklin E. E., 2005, *Astronomische Nachrichten*, **326**, 964
- Farihi J., Becklin E. E., Zuckerman B., 2008, *ApJ*, **681**, 1470
- Farihi J., Gänsicke B. T., Koester D., 2013, *MNRAS*, **432**, 1955
- Friedrich S., Zinnecker H., Correia S., Brandner W., Burleigh M., McCaughrean M., 2007, in Napiwotzki R., Burleigh M. R., eds, *Astronomical Society of the Pacific Conference Series* Vol. 372, 15th European Workshop on White Dwarfs. p. 343 ([arXiv:astro-ph/0611511](https://arxiv.org/abs/astro-ph/0611511))
- Gaia Collaboration et al., 2016, *A&A*, **595**, A1
- Gaia Collaboration et al., 2018, *A&A*, **616**, A1
- Gänsicke B. T., Schreiber M. R., Toloza O., Fusillo N. P. G., Koester D., Manser C. J., 2019, *Nature*, **576**, 61
- Gianninas A., Bergeron P., Ruiz M. T., 2011, *ApJ*, **743**, 138
- Gilliland R. L., et al., 2000, *ApJL*, **545**, L47
- Gould A., Kilic M., 2008, *ApJ*, **673**, L75
- Guenther E. W., Paulson D. B., Cochran W. D., Patience J., Hatzes A. P., Macintosh B., 2005, *A&A*, **442**, 1031
- Hogan E., Burleigh M. R., Clarke F. J., 2011, in Schuh S., Drechsel H., Heber U., eds, *American Institute of Physics Conference Series* Vol. 1331, *American Institute of Physics Conference Series*. pp 271–277 ([arXiv:1102.0506](https://arxiv.org/abs/1102.0506)), doi:10.1063/1.3556210
- Kalirai J. S., Marigo P., Tremblay P.-E., 2014, *ApJ*, **782**, 17
- Kennedy G. M., Kenyon S. J., 2008, *ApJ*, **673**, 502
- Keppler M., et al., 2018, *A&A*, **617**, A44
- Kopytova T. G., Brandner W., Tognelli E., Prada Moroni P. G., Da Rio N., Röser S., Schilbach E., 2016, *A&A*, **585**, A7
- Kovács G., et al., 2014, *MNRAS*, **442**, 2081
- Krist J. E., Hook R. N., Stoehr F., 2011, in *Optical Modeling and Performance Predictions V*. p. 81270J, doi:10.1117/12.892762
- Lafrenière D., Marois C., Doyon R., Nadeau D., Artigau É., 2007, *ApJ*, **660**, 770
- Lagrange A.-M., et al., 2009, *A&A*, **493**, L21
- Lagrange A. M., et al., 2010, *Science*, **329**, 57
- Leinert C., Zinnecker H., Weitzel N., Christou J., Ridgway S. T., Jameson R., Haas M., Lenzen R., 1993, *A&A*, **278**, 129
- Livingston J. H., et al., 2018, *AJ*, **155**, 115
- Luhman K. L., Burgasser A. J., Bochanski J. J., 2011, *ApJ*, **730**, L9
- Macintosh B., et al., 2015, *Science*, **350**, 64
- Mann A. W., et al., 2016, *ApJ*, **818**, 46
- Marois C., Macintosh B., Barman T., Zuckerman B., Song I., Patience J., Lafrenière D., Doyon R., 2008, *Science*, **322**, 1348

- Marois C., Zuckerman B., Konopacky Q. M., Macintosh B., Barman T., 2010, *Nature*, **468**, 1080
- Müller M., Weigelt G., 1987, *A&A*, **175**, 312
- Mustill A. J., Villaver E., Veras D., Bonsor A., Wyatt M. C., 2013, in *European Physical Journal Web of Conferences*. p. 06008, doi:10.1051/epjconf/20134706008
- Nielsen E. L., et al., 2019, *AJ*, **158**, 13
- Nordhaus J., Spiegel D. S., 2013, *MNRAS*, **432**, 500
- Pasquini L., Pala A. F., Ludwig H. G., Leao I. C., de Medeiros J. R., Weiss A., 2019, *A&A*, **627**, L8
- Paulson D. B., Saar S. H., Cochran W. D., Henry G. W., 2004, *AJ*, **127**, 1644
- Perrot C., Baudoz P., Boccaletti A., Rousset G., Huby E., Clénet Y., Durand S., Davies R., 2018, *arXiv e-prints*, p. arXiv:1804.01371
- Perryman M., 2018, *The Exoplanet Handbook*
- Perryman M. A. C., et al., 1998, *A&A*, **331**, 81
- Reffert S., Bergmann C., Quirrenbach A., Trifonov T., Künstler A., 2015, *A&A*, **574**, A116
- Röser S., Schilbach E., Piskunov A. E., Kharchenko N. V., Scholz R.-D., 2011, *A&A*, **531**, A92
- Salaris M., Bedin L. R., 2018, *MNRAS*, **480**, 3170
- Sato B., et al., 2007, *ApJ*, **661**, 527
- Schilbach E., Röser S., 2012, *A&A*, **537**, A129
- Shabram M. I., et al., 2020, *AJ*, **160**, 16
- Spiegel D. S., Burrows A., 2012, *ApJ*, **745**, 174
- Tremblay P.-E., Schilbach E., Röser S., Jordan S., Ludwig H.-G., Goldman B., 2012, *A&A*, **547**, A99
- Vanderburg A., et al., 2018, *AJ*, **156**, 46
- Vanderburg A., et al., 2020, *arXiv e-prints*, p. arXiv:2009.07282
- Veras D., Evans N. W., Wyatt M. C., Tout C. A., 2014, *MNRAS*, **437**, 1127
- Vigan A., et al., 2020, *arXiv e-prints*, p. arXiv:2007.06573
- Villaver E., Livio M., 2009, *ApJ*, **705**, L81
- Xu S., Ertel S., Wahhaj Z., Milli J., Scicluna P., Bertrang G. H. M., 2015, *A&A*, **579**, L8
- Xu S., Dufour P., Klein B., Melis C., Monson N. N., Zuckerman B., Young E. D., Jura M. A., 2019, *AJ*, **158**, 242
- Zinnecker H., Friedrich S., 2001, in Schielicke E. R., ed., *Astronomische Gesellschaft Meeting Abstracts Vol. 18*, *Astronomische Gesellschaft Meeting Abstracts*.
- Zinnecker H., Kitsionas S., 2008, in Fischer D., Rasio F. A., Thorsett S. E., Wolszczan A., eds, *Astronomical Society of the Pacific Conference Series Vol. 398*, *Extreme Solar Systems*. p. 155
- Zinnecker H., Correia S., Brandner W., Friedrich S., McCaughrean M., 2006, in Aime C., Vakili F., eds, *IAU Colloq. 200: Direct Imaging of Exoplanets: Science & Techniques*. pp 19–24, doi:10.1017/S1743921306009021
- Zuckerman B., Becklin E. E., 1987, *ApJ*, **319**, L99
- Zuckerman B., Melis C., Klein B., Koester D., Jura M., 2010, *ApJ*, **722**, 725
- Zuckerman B., Xu S., Klein B., Jura M., 2013, *ApJ*, **770**, 140
- van Saders J. L., Gaudi B. S., 2011, *ApJ*, **729**, 63
- von Hippel T., 1998, *AJ*, **115**, 1536

This paper has been typeset from a $\text{\TeX}/\text{\LaTeX}$ file prepared by the author.